# Tunable broadband antireflection structures for silicon at terahertz frequency

Y. W. Chen, P. Y. Han, and X.-C. Zhang[a)]
*Center for THz Research, Rensselaer Polytechnic Institute, Troy, New York 12180, USA*

(Received 7 December 2008; accepted 6 January 2009; published online 26 January 2009)

We report enhanced transmission of broadband terahertz electromagnetic waves in the frequency range from 0.2 to 3.15 THz using silicon with micropyramid surface structures. We observe a maximum 89% reduction in reflectivity of terahertz power when the sample with 60-$\mu$m-period micropyramids is used, compared to a planar silicon substrate. By varying the period of micropyramid structures from 110 to 30 $\mu$m, the cutoff frequency of enhanced transmission is tuned from 0.74 to 2.93 THz and the bandwidth of enhancement increases from 0.91 to 3.15 THz, respectively. © *2009 American Institute of Physics*. [DOI: 10.1063/1.3075059]

Silicon, especially high-resistivity silicon, is widely used in terahertz components due to its broadband transparent window spanning from microwave to midinfrared.[1] Its range of application spans from windows and lenses to filters and beam splitters. However, because of its high dielectric constant, silicon is usually associated with high Fresnel reflection loss (30% in terahertz power from a single surface) and possibly limiting spectral resolution stemming from the finite time window imposed by the strong secondary reflections from its surfaces. To improve system performance, it is of great importance to reduce the reflection at the air-silicon interface to increase dynamic range and improve spectral resolution.

Antireflection (AR) coatings for silicon at terahertz frequency have been implemented in several ways. One method was to use a quarter-wave thin film as the AR layer, which had a refractive index of $n=\sqrt{n_{\text{silicon}}}$.[2] This method was only suited for narrowband and inadequate for broadband terahertz time-domain spectroscopy (TDS). Silicon nanotips were reported as another AR coating method, whose improvement of transmission was limited to frequencies higher than 1 THz.[3] Photonic crystal slabs made with air holes in silicon were also illustrated to enhance transmission from 0.1 to 0.45 THz with performance at higher frequencies dramatically deteriorated.[4] Multilayer coatings were used for broadband AR.[5,6] Usually the design and fabrication process was complicated due to the lack of materials, which had low absorption and suitable refractive index. Subwavelength surface relief structures were recently employed to implement enhanced transmission,[7–10] which enhanced zero-order diffraction by using surface structures smaller than terahertz wavelengths.

In this paper, we demonstrate reduction in reflection of terahertz waves using subwavelength micropyramid structures at the silicon surface. This method utilizes the property of a medium with continuously changing refractive index. The micropyramid structure can be thought as the composition of many extremely thin layers whose refractive index is dependent on the area ratio of silicon and air. Thus, the effective refractive index of the AR medium continuously changes from 3.4 in the silicon substrate to 1 in air. The result is a great reduction in reflection due to better impedance matching between silicon and air.

In the experiment, crystallographic wet etching was employed for the fabrication of AR components. 25% tetramethylammonium hydroxide with surfactant was used as an etching solution. The etching was crystallographic as the etch rate in ⟨100⟩ direction was 6 times faster than that in the ⟨110⟩ direction and 60 times faster than that in the ⟨111⟩ direction, which produced square micropyramid with an apex angle of 72° formed by four ⟨111⟩ planes.[11,12] We fabricated five different samples with micropyramid periods of 110, 75, 60, 45, and 30 $\mu$m. Figure 1 shows the scanning electron microscopy (SEM) image of a sample with 45-$\mu$m-period micropyramid surface structures.

A terahertz-TDS was used to demonstrate the AR performance of the silicon samples with various one-sided micropyramid surface structures. The results were compared with that of a planar silicon substrate. The available spectra spanned from 0.2 to 4 THz using a GaP crystal sensor. Planar silicon substrate and samples with AR structures were positioned in terahertz beam path with normal incidence. The structured surface is facing the incident terahertz beam and almost the same performance is observed when the other side is facing the incident terahertz beam. The relative transmission spectra of the terahertz field were calculated as terahertz amplitude spectra through the samples divided by that through planar silicon substrate. Figure 2 shows the experimental results as scattered symbols. Silicon samples with micropyramid periods from 110 to 30 $\mu$m have relative

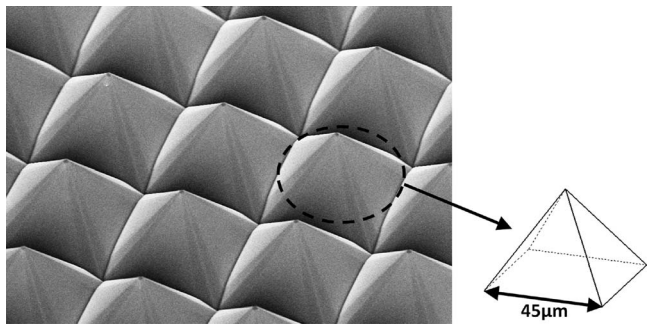


FIG. 1. SEM image of silicon surface with 45-$\mu$m-period micropyramid structures.

a)Author to whom correspondence should be addressed. Electronic mail: zhangxc@rpi.edu.

 

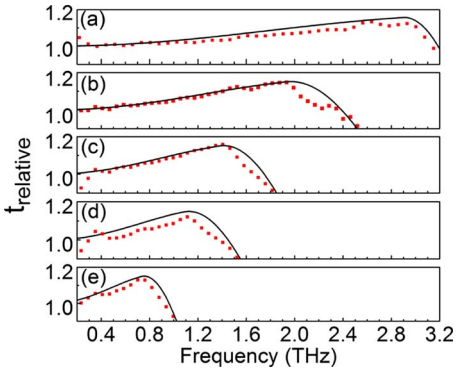


FIG. 2. (Color online) Relative transmission amplitude ($t_{relative}$) of micropyramid structured samples with periods (a) 30, (b) 45, (c) 60, (d) 75, and (e) 110 $\mu$m. Experimental and simulation results are shown by the scattered symbols and solid lines, respectively.

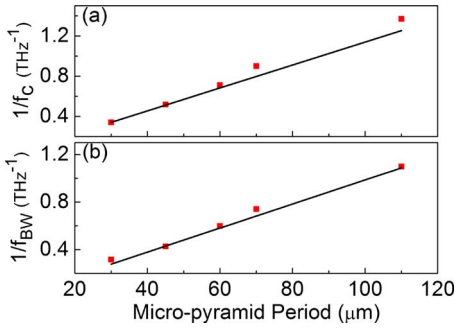


FIG. 3. (Color online) Reciprocals of cutoff frequency ($f_C$) and bandwidth ($f_{BW}$) of micropyramid structured samples as a function of periods. Experimental results are shown as scattered symbols. Calculated results of $1/f_C$ and simulation results of $1/f_{BW}$ are shown in straight lines.

transmission peak amplitudes of 1.13, 1.12, 1.16, 1.15, and 1.13 respectively. The peaks of relative transmission are located at 0.75, 1.11, 1.41, 1.93, and 2.93 THz, respectively. As observed from Fig. 2, silicon samples with smaller periods have larger AR bandwidth. Samples with micropyramid periods from 110 to 30 $\mu$m have AR bandwidths of 0.91, 1.35, 1.67, 2.34, and 3.15 THz, respectively.

To understand the AR effect of micropyramid structures, we used the graded index method to simulate the impedance matching between air and silicon substrate. Each layer in the pyramid was considered to have an effective refractive index of $n_{\text{eff}}=\sqrt{f\times 3.4^2+(1-f)\times 1^2}$, where $f$ is the filling factor (area fraction) of silicon in each layer.[13] During matrix calculation, each layer was represented by a propagation matrix $P_{(i)}$. Each interface between adjacent layers was represented by a transmission matrix $M_{(i-1)}$. The overall transmission matrix $M$ was written as $P_{(1)}\Pi_{i=2}^{n}M_{(i-1)}P_{(i)}$ in which $n$ is the number of layers, and $P_{(n)}$ and $P_{(1)}$ are the transmission matrices for silicon and air, respectively. The transmission and reflection of the system were obtained by converting the transmission matrix $M$ into scattering matrix $S$. When the number of layers was greater than 500, the simulation result converged. Based on the calculation, the relative transmission amplitude approached a maximum value of 1.194 for all micropyramid structures without considering diffraction. In this case, a relative field transmission amplitude of 1.194 was equivalent to zero reflectivity, giving an upper limit on the performance of these AR silicon samples. The AR effect was mainly determined by the height of the pyramid, which was related to the pyramid period by $h=(\Lambda/2)\tan 54.7°$, where $\Lambda$ is the period of the micropyramid. For consistency, we discuss AR effect as a function of period throughout this paper.

Diffraction effect strongly influences terahertz transmission of these samples when their pyramid periods approach the order of terahertz wavelength. As a result, each micropyramid structured sample has its specific peak AR frequency, above which diffraction reduces the transmitted terahertz field (zero order diffraction). This frequency is named as the cutoff frequency and can be calculated by the expression of $f_C=c/(\Lambda n)$, where $c$ is the speed of light and $n$ is the refractive index of silicon. In our simulation, we applied an analytical diffraction function, $\text{sinc}[(f-fc)/a]$ to the AR simulation of each micropyramid structure, where $a$ is a fitting parameter. Solid lines in Fig. 2 represent the simulated curves of relative transmission of each sample. The simulated curves fit the experimental data well.

Figure 3(a) plots the reciprocal of measured cutoff frequency versus micropyramid period as scattered symbols. It has a well-defined linear dependency on pyramid period. Experimental results agree well with the calculated ones (straight line) using the equation above. Furthermore, each micropyramid structured sample has a particular bandwidth of AR effect. Figure 3(b) illustrates the reciprocal of the measured bandwidth against micropyramid period as scattered symbols. The experimental results show a linear dependency on pyramid period and are reproduced by simulation (straight line) very well.

To directly demonstrate the reflection performance of micropyramid structured samples, we plot the reflectivity for all samples. Figure 4 shows the absolute power reflectivity of each AR sample and planar silicon. It was obtained by considering reflection and transmission from both surfaces of the silicon sample and using the data in Fig. 2. Micropyramid structures with greater height has better AR effect at lower frequencies, but starts to roll off more quickly because of diffraction. For example, a 60-$\mu$m-period sample has a minimum reflectivity of 3% at 1.41 THz, corresponding to a maximum reduction in reflectivity by 89% when comparing with planar silicon. However, its AR effect retrogrades beyond 1.67 THz. The 30-$\mu$m-period sample exhibits the best overall AR effect and displays superior AR performance over a broad frequency range. In general the maximum reduction in power reflectivity is over 80% for most samples, compared to planar silicon.

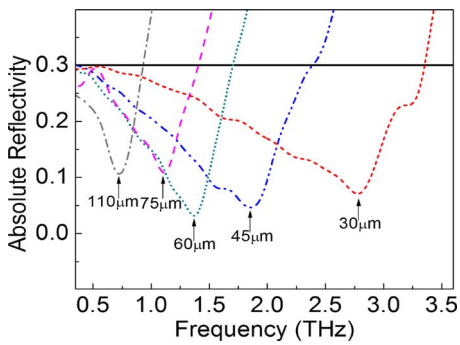


FIG. 4. (Color online) Power reflectivity is plotted for samples with various micropyramid structure periods. Reflectivity of planar silicon is shown by the solid line.

AR design with crystallographic wet etched micropyramid surface structures has many unique advantages. The fabricated samples are polarization independent at normal incidence. From our experimental results, the terahertz amplitude virtually stayed the same as the azimuthal angle is rotated from 0° to 360°. Additionally, the samples are mostly independent of incident angle below 20°. Furthermore, the size of pyramid can be precisely tuned to control the bandwidth and cutoff frequency. The size of pyramid is of the order of tens of microns and does not alter the silicon substrate too much. Finally, optimization of the pyramid period may result in broader spectra of enhanced transmission.

In conclusion, silicon with micropyramid surface structures fabricated by crystallographic wet etch have been demonstrated with tunable and broadband AR performance. The frequency range with enhanced transmission spans from 0.2 to 3.15 THz, which may be further increased by tuning the parameter of the pyramid. The maximum reduction in reflectivity is more than 89%, which is achieved using the sample with a micropyramid period of 60 $\mu$m. Future work will focus on exploration of optimum pyramid design for best overall performance.

The authors would like to thank Bryant Colwill, Kent Way, Nicholas Karpowicz and Jingle Liu for valuable discussion. Y.W.C. is funded by the National Science Foundation IGERT Program under Grant No. 0333314. This work is supported by the Army Research Office under Grant No. W911NF-07-1-0278.

[1] D. Grischkowsky, S. Keiding, M. van Exter, and Ch. Fattinger, J. Opt. Soc. Am. B **7**, 2006 (1990).
[2] C. R. Englert, M. Birk, and H. Maurer, IEEE Trans. Geosci. Remote Sens. **37**, 1997 (1999).
[3] Y. Huang, S. Chattopadhyay, Y. Jen, C. Peng, T. Liu, Y. Hsu, C. Pan, H. Lo, C. Hsu, Y. Chang, C. Lee, K. Chen, and L. Chen, Nat. Nanotechnol. **2**, 770 (2007).
[4] T. Prasad, V. L. Colvin, and D. M. Mittleman, Opt. Express **15**, 16954 (2007).
[5] I. Hosako, Appl. Opt. **44**, 3769 (2005).
[6] D. Poitras and J. A. Dobrowolski, Appl. Opt. **43**, 1286 (2004).
[7] C. Bruckner, B. Pradarutti, O. Stenzel, R. Steinkopf, S. Riehemann, G. Notni, and A. Tunnermann, Opt. Express **15**, 780 (2007).
[8] S. Kuroo, K. Shiraishi, H. Sasho, H. Yoda and K. Muro, CLEO (Optical Society of America, Washington, DC, 2008), Paper No. CThD7.
[9] A. Thoman, A. Kern, H. Helm, and M. Walther, Phys. Rev. B **77**, 195405 (2008).
[10] C. Bruckner, T. Kasebier, B. Pradarutti, S. Riehemann, G. Notni, E. Kley, and A. Tunnermann, *33rd Int. Conf. on Infrared, Millimete, and Teraherz Waves (IRMMW-THz)*, 2008, Paper No. F2K4.1485.
[11] E. Bassous, IEEE Trans. Electron Devices **25**, 1178 (1978).
[12] D. Resnik, D. Vrtacnik, R. Alkancic, M. Mozek, and S. Almon, J. Micromech. Microeng. **15**, 1174 (2005).
[13] L. Escoubas, J. J. Simon, M. Loli, G. Berginc, F. Flory, and H. Giovanni, Opt. Commun. **226**, 81 (2003).